International Journal of Computing and Digital Systems
ISSN (2210-142X)
Int. J. Com. Dig. Sys. , No. (Mon-20..)

http://dx.doi.org/10.12785/ijcds/XXXXXX

Advanced Heterogeneous Ensemble Voting Mechanism with GRFOA based Feature Selection for Emotion Recognition from EEG Signal Analysis

Rajanikanth Aluvalu[1], V. Asha[2], R J Anandhi[2], MVV Prasad Kantipudi[3], Jyoti Bali[4] and Mousumi Bhanja[3]

[1]*Chaitanya Bharathi Institute of Technology, Hyderabad, India*
[2]*New Horizon College of Engineering, Ring Road, Bellandur Post, Bengaluru- 560103*
[3]*Symbiosis Institute of Technology, Symbiosis International (Deemed University), Pune 412115, Maharashtra, India*
[4]*School of Computing, MIT Vishwaprayag University*

Received Mon. 20, Revised Mon. 20, Accepted Mon. 20, Published Mon. 20

Abstract: Important features of electroencephalogram (EEG) that underlie emotional brain processes include high temporal resolution and asymmetric spatial activations. Unlike voice signals or facial expressions, which are easily duplicated, EEG-based emotion documentation has shown to be a reliable option. Because people react emotionally differently to the same stimulus, EEG signals of emotion are not universal and can vary greatly from one individual to the next. As a consequence, EEG signals are highly reliant on the individual and have shown promising results in subject-dependent emotion identification. The research suggests using ensemble learning with an advanced voting mechanism to understand the spatial asymmetry and temporal dynamics of EEG for accurate and generalizable emotion identification. Using VMD (Variational-Mode-Decomposition) and EMD (Empirical mode decomposition), two feature extraction techniques, on the pre-processed EEG data. When selecting features, the Garra Rufa Fish optimization algorithm (GRFOA) is employed. The ensemble model includes a Temporal Convolutional Network (TCNN), an Extreme Learning Machine (ELM), and a Multi-Layer Perception Network (MLP). The proposed method involves utilizing EEG data from individual subjects for training classifiers, enabling the identification of emotions. The result is then derived via a voting classifier that is based on heterogeneous ensemble learning. Two publicly obtainable datasets, DEAP and MAHNOB-HCI, are used to validate the proposed approach using broader cross-validation settings.

Keywords: Empirical Mode decomposition; Electroencephalogram; Garra Rufa Fish optimization algorithm; Extreme Learning Machine; Emotion analysis; Multi-Layer Perception Network.

1. INTRODUCTION

Along with more conventional methods, such as affective reports (e.g. SAM), bio-signals have lately grown in popularity as a means of gauging emotional states. Emotion identification has long made use of bio-signals such as respiration, galvanic skin reaction, phalanx temperature, ECG, electrooculographic (EOG) signals, blood volume pulse, and cerebral blood flow [1]. A number of recent studies have concentrated on the analysis of brain signals using methods like functional near-infrared spectroscopy (fNIRS), electroencephalograms (EEGs), event-related optical signals (EROS), and proton emission tomography (PET) [2]. When associated to the other technologies listed, EEG delivers superior temporal resolution.

The market is seeing growth due to the increasing demand for brain-computer interfaces (BCIs), particularly for BCI applications that address brain illnesses and accidents. The global BCI market was worth $1,488,000,000$ in 2020 [3]. With a projected CAGR (Compound Annual Growth Rate) of 13.9% from 2021–2030, its value is anticipated to reach $5,463,000,000,000,000 by 2030. Getting the signal recording out of clinical research labs has been a big obstacle in EEG system development recently [4]. Typically, subjects were monitored in hospital or laboratory settings using bulky technology. The development of wearable electroencephalogram (EEG) equipment, however, has opened the door to non-invasive, long-term monitoring of brain signals in settings other than laboratories [5]. As a result, BCI may be used for emotion identification in several domains, thanks to the increasingly wearable prototype solutions. The

E-mail address: author 1, author 2, author 3

non-clinical use of EEG is extensive in neuromarketing for the purpose of gauging consumer responses to offerings [6]. Prior research in this area has made use of a variety of commercially available EEG equipment.

A person's emotional state may be defined as their bodily and mental reactions to significant life events, whether those events occur within or outside of themselves [7]. The bond between people and their natural surroundings is enhanced. There are essentially three ways that machines get emotional data, all based on how humans see the world. One approach is to use visual cues such as gaze, posture, gestures, and lip and face movements to identify emotions [8]. Two, one may use the pitch, length, and strength of one's voice to create an emotional classification system. A third category includes systems that detect emotions by analyzing biochemical cues [9]. Emotion detection using facial expressions or auditory signals has proved successful, but physiological signals, which are unconscious displays of emotions, have the advantage of being impossible to hide or cover, even after training. As a result, researching physiological signal properties and applying them to emotion identification is a worthwhile endeavor [10].

Many models exist for representing emotions; the two most prevalent are the dimensional model and the discrete perfect. There are six primary emotions represented by the discrete model: joy, sorrow, wrath, surprise, disgust, and fear [11]. From these fundamental emotions, all other emotions emerge. A valence-arousal 2-dimensional table represents emotions in the dimensional model. The valence is a measure of the degree to which an feeling is happy or sad. The arousal level, which can range from calm to excited, is a measure of how active a person is [12]. Also, technology for acquiring EEG signals while exercising and other electrodes has evolved over time thanks to the ongoing development of 60-acquisition equipment, such as noncontact skin electrodes [13]. We are able to capture EEG waves precisely and undisturbed. Among them, the International 10-20 Standard is most often used to determine where to place EEG electrodes. New developments in the area of EEG signals, especially in emotion documentation, have been spurred by advancements in data collecting technologies [14].

There are over 70 components to EEG emotion recognition. Part one involves processing EEG data, which involves doing things like extracting features and removing noise and artifacts from the raw signal. Common space modeling, independent component analysis, principal component analysis, filters, and other approaches are often used to eliminate these false signals [15]. To remove the artifacts while keeping the original characteristics, one might employ a fusion signal processing approach. Emotion recognition has been under research for a while, however there are still issues. To start, when it comes to EEG signals, the majority of approaches still don't take cross-subject research into account and instead concentrate on subject-dependent investigations. Secondly, as compared to deep learning's performance in picture classification, the accuracy of emotion categorization is significantly lower. As a result, EEG emotion identification is an area that might greatly benefit from deep learning techniques. Third, many approaches exploit just one of the numerous properties present in EEG data, rather than fusing them together [16]. As a fourth point, emotions have a role in the connection between channels. It is worthwhile to investigate how this relationship might be utilized to enhance the precision of mood categorization, as certain systems fail to consider it.

For EEG data, this study employs an ensemble classifier, a GRFOA model for feature selection, and EMD and VMD for feature extraction. In order to validate the ensemble classifier for analysis, an advanced voting method is employed. In terms of different metrics, the tests are conducted using datasets that are publicly available. Here is the breakdown of the residual sections of the paper: Section 2 provides a bibliography of pertinent literature; Section 3 presents the model under consideration; Section 4 delves into an examination of the findings; and Section 5 draws a conclusion.

2. Related Works

We suggest building a robust hierarchical Bayesian spectral using the hierarchical Bayesian ensemble techniques, building on the work of Yang et al. [17] to enhance the graph-based regression models' robustness. By utilizing a data-driven adaptive modification method to model parameters, the suggested HB-SR is able to significantly mitigate the effects of noise. In particular, the present study takes use of three distinct distributions the Student t, the Laplace, and the Gaussian to improve the HB-SR's generalizability. We performed experiments using emotional EEG data to objectively assess the HB-SR framework's performance. Experimental findings have repeatedly shown that the proposed HB-SR outperforms previous spectral regression algorithms in terms of noise suppression and robust EEG emotion identification.

In order to enhance emotion recognition, Asif et al. [18] want to create a generic model that represents emotions in a fuzzy VAD space. To better describe emotions, we created a fuzzy VAD space by dividing the crisp VAD space into low, medium, dimensions. In order to identify emotions, a system has been created that combines EEG data with fuzzy VAD space. Using time-frequency spectrograms to extract spatial and temporal feature vectors, we analyzed the EEG characteristics and also took into account the subjects' stated VAD values. The DENS dataset, which comprises subjective assessments, EEG data, and twenty-four distinct emotions, was used for the investigation. A number of models based were used to verify the study inside the deep fuzzy framework. The corresponding emotion identification accuracy for the 24 emotion classes was 96.09%, 95.75%, and 95.31%, as a consequence of these models. Two ablation studies were also included of the research; one used

crisp VAD space and the other did not. In contrast to the two models, the deep fuzzy framework produced superior results when applied to crisp VAD space. Extending the model to forecast emotions across subjects yielded encouraging findings with a 78.37% accuracy rate, demonstrating the technique's generalizability. Affective computer interaction, and mental health monitoring are just a few of the real-world domains that could benefit from the created model's general character and good cross-subject predictions.

To overcome these shortcomings, Li et al. [19] suggested a multi-view EEG-based emotion recognition, which helps to automatically features while minimizing individual differences. Initially, the raw EEG signals are processed using the short-time Fourier transform (STFT) to extract differential entropy (DE) components. Second, at the level of the EEG time-frame, the discriminative emotional information is aggregated by treating each DE feature channel as a view and applying the attention processes at distinct views. To extract nonlinear interactions across time intervals, is used. To further investigate the possibility of complimentary information across various perspectives and improve the feature's representational capabilities, features from several channels are fused using a feature-level fusion. Lastly, in order to reduce individual variance, domain-invariant features are generated using a domain discriminator. This feature projection merges data from both domains into a single data representation space. Two publicly available datasets, SEED and DEAP, were used to assess our suggested approach. We found that our CADD-DCCNN approach performed better than the SOTA methods in our experiments.

In order to improve ER's capacity for feature extraction, Akhand et al. [20] suggest a connection feature map (CFM) that makes advantage of partial mutual information (PMI) through the addition of a third channel. For every set of EEG channels, the suggested method determines PMI-based connectivity characteristics and displays CFM in two and three dimensions. When it comes to 2D and 3D CFMs, the Convolutional Neural Network (CNN) is the way to go for emotion classification. Extensive testing has been carried out on the DEAP benchmark EEG dataset to create CFMs from EEG signals. The improved CFM outperformed the previous comparable modern approaches, as revealed by PMI's extra information, and it delivered superior ER presentations than the one that used normal MI or NMI.

A new method has been proposed by Farokhah et al. [21] that uses EEG signals to choose channels based on biological information. Time and frequency domain data are used to categorize the brain into different groups and subgroups, and the capability of the channels linked to those groups is then determined. Based on the accuracy results generated by the support vector machines (SVM), we can tell which of these groups and subgroups has the potential to perform better. By comparing the chosen channels'-led classification approaches to a deep learning model for valence and arousal classes, we were able to ascertain the channels' capacity for correct classification. The DEAP dataset is used to verify the technique, showing that it has the ability to improve the efficiency and accuracy of EEG-based emotion categorization. This novel approach to EEG research holds great promise for the future, as it streamlines the setup process, allows for customization according to the emotions being studied, and achieves the highest levels of accuracy (95.7% for intra-subject and 94.65% for cross-subject emotion classification on average).

To fill this need, Blanco-Rios et al., [22] suggests using technology to enhance humanities education and encourage the growth of new approaches to teaching the subject. More specifically, they suggest using immersive learning environments to track students' emotional states as they progress through the course. To get there, we built an EEG-based system that can identify and categorize emotions in real time. Feelings of awe, love, hatred, want, happiness, and melancholy were in line with the first suggestion put out by Descartes (Passions). With the goal of building a thorough and engaging learning environment, this system intends to incorporate platform. Every five seconds, the authors of this study estimated the levels of valence, arousal, and dominance (VAD) using a machine learning (ML) emotion recognition model. The top 8 channels and their corresponding band powers were extracted using PCA, PSD, RF, and Extra-Trees. Additionally, shift-based data division and cross-validations were used to assess different models. In comparison to the 88% accuracy stated in the literature, Extra-Trees attained a general accuracy of 96% after evaluating their performance. After some tweaks, the suggested model could now categorize Descartes' six primary passions and provide real-time predictions of VAD variables. The VAD values, however, allow for the classification of more than fifteen emotions (as documented in VAD emotion mapping), thereby expanding the scope of this application.

In a simulated driving situation, Chen et al., [23] have proposed an EEG collection and emotion categorization system. To model obstacle avoidance at varying degrees of risk, the approach makes use of vehicle speed as an independent variable. In order to process the data, it employs graph neural networks (GNN) that mimic the brain's physiological architecture through functional connection and attention processes. The characteristics were also compared from an entropy and power standpoint through a battery of experiments. The highest F1 score for a single label was 76.7%, while the three-class classification result was 75.26 percent. The highest F1 score for a single label was 91.86%, contributing to the overall binary classification result of 91.5%. With the help of deep learning models, the solution was able to successfully mimic a variety of risky scenarios, record the driver's electroencephalogram (EEG), and keep tabs on their emotional state.

Using an enhanced capsule network, Fan et al. [24] presented a two-module approach to EEG emotion identifi-

cation. When learning specific EEG spatial representations, it is more favorable to use an enhanced capsule network as the spatial module. In order to improve the model's classification capabilities, the ResLSTM module takes information flow from the upper spatial module and uses residual connections to learn complementary features of the spatiotemporal dual module. This results in more discriminative EEG features. Arousal, valence, and dominance all achieved average accuracy levels of 98.06%, 97.94%, and 98.15% on the DEAP dataset, respectively. On average, the DREAMER dataset achieved arousal accuracy of 94.97%, valence accuracy of 94.71%, and dominance accuracy of 94.96%. We found that our strategy is more effective than the current best practices.

A new method called CS-GAN, as up by Chang et al. [25], can improve cross-subject emotion identification by creating EEGs of listeners in reaction to a speaker's voice. We trained generative adversarial networks (GANs) to produce EEGs that were generated by stimuli by first establishing a mapping connection between speech and EEGs. In addition, we improved the produced EEGs' fidelity and variety by including the GAN-based EEG generating approach. In order to determine the various emotional categories expressed in the speech, the produced EEGs were then analyzed with a CNN-LSTM model. To make the approach work better across subjects, we averaged the EEGs and got the event-related potentials (ERPs). In cross-subject emotion detection tasks, the experimental findings show that the produced EEGs using this technology surpass genuine listener EEGs by 9.31%. In addition, the ERPs demonstrate a 43.59% improvement, proving that this approach is useful in recognizing emotions across subjects.

On this topic, Yuvaraj et al. [26] compared the effectiveness of several EEG feature sets in classifying emotional states according to valence and arousal. We looked at the stats, fractal dimension (FD), and wavelet-derived EEG feature sets to see how well they classified data. Five separate and publicly accessible datasets were used to assess performance: DREAMER. The classifier techniques used were support vector machine (SVM). Mean valence classification accuracy was 85.06% and mean arousal classification accuracy was 84.55% for the five datasets that were considered using the FD-CART feature-classification approach. Emotion identification using FD features obtained from EEG data is dependable, since these results are stable across all five datasets. An online feature extraction framework may be built using the data, which would pave the way for a real-time emotion identification system based on electroencephalograms.

To enhance EEG data categorization, Dutta et al., [27] has utilized a multilayer perceptron artificial neural network (MLP-ANN) in conjunction with long short-term memory (LSTM). From 640 datasets acquired using a Muse EEG-powered headband equipped with a global EEG position standard, they made their selection. To improve the performance of the LSTM and MLP-ANN algorithms, we employed five distinct activation function combinations with two best loss model operations and an Adam optimizer. The "EEG Brainwave Dataset: Feeling Emotions" database on Kaggle was used to train the DL classification model with various statistical parameters. We examined the matrix limits of both DL models. The findings demonstrate that the binary cross-entropy loss model obtained the highest accuracy, while the logcosh loss model of the MLP-ANN model achieved the lowest accuracy.

To obtain an outstanding classification impact, Wang et al., [28] suggests a deep l identification that fuses electroencephalogram (EEG) inputs with facial expressions. The face features are first extracted from the expressions using a pre-trained convolution neural network (CNN). To extract even more important elements from the face frame, the attention mechanism is then developed. Afterwards, convolutional extract spatial characteristics data. These CNNs learn the features of the left and right hemisphere channels EEG channels using a global and a local convolution kernel, respectively. The classifier is trained to recognize emotions using the fused features of facial expressions and electroencephalograms (EEGs), following feature-level fusion. In order to test how well the suggested model worked, this study used datasets. The DEAP dataset has a valence dimension classification accuracy of 96.63% and an classification accuracy of 97.15%; the MAHNOB-HCI dataset has an accuracy of 96.69% and an accuracy of 96.26%. The suggested model is able to accurately identify emotions, according to the experimental data.

In order to identify human emotions from EEG waves, Iyer et al. [29] suggests a new approach. We have taken into account three different negative. In order to calculate the differential entropy, the EEG data are first divided into five frequency bands based on the EEG rhythms. For precise emotion recognition, a hybrid model is created Additionally, all three models for emotion recognition are given the retrieved information. The last step is an ensemble model that takes the best parts of each model and uses them together. Two datasets, SEED and DEAP, for EEG-based emotion analysis, validate the projected method. When tested on the SEED dataset for emotion categorization, the created approach attained an accuracy of 97.16 percent. The suggested method outperforms the alternatives for EEG-based emotion analysis, according to the experimental data.

3. Proposed system

In order to derive intrinsic mode functions (IMF) from EEG data, the suggested technique employs variational. A pair of characteristics, the IMF's Peak Power Spectral Density and the signal's First Difference, are computed for every IMF before being inputted into an ensemble classifier for the purpose of classification.

A. EEG data

For a number of reasons, researchers choose electroencephalography (EEG) over other non-invasive methods of

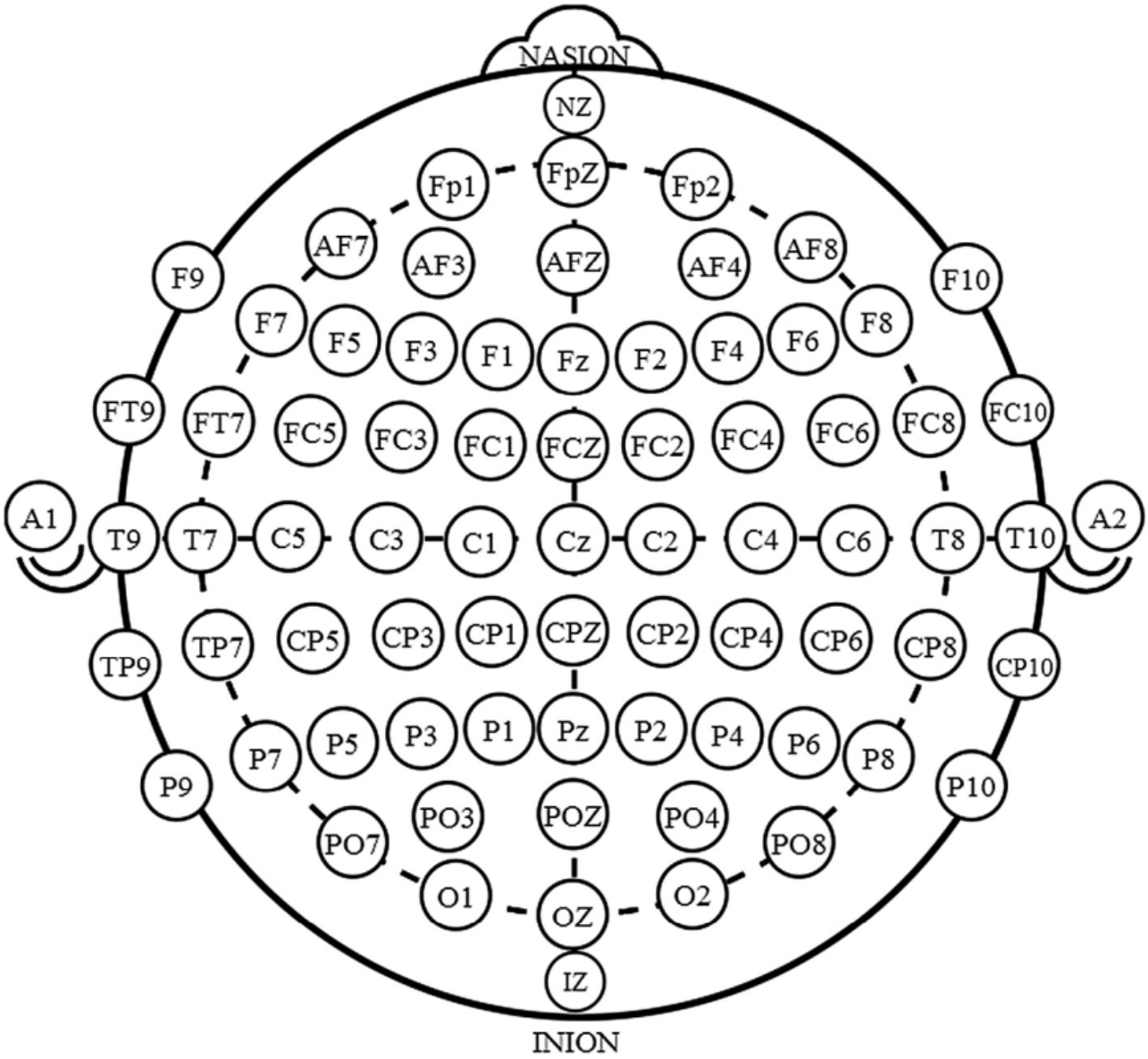

Figure 1. 10–20 Electrode-Placement system [30]

monitoring brain electrical activity along the scalp. Recognizing human emotions is one of such uses. The typical range of frequencies for an electroencephalogram (EEG) signal is between 1 Hz and 100 Hz, and its amplitude can be anywhere from 10 mV to 100 mV. The five primary frequency bands found in electroencephalograms (EEGs) are as follows: the delta band, which is below 4 Hz, the theta band, which is among 14 and 40 Hz, and the band, which is 40 Hz or higher.

Both bipolar and monopolar recording techniques are available for EEG signals. The voltage differential between the scalp electrode and the reference electrode, which is located in the ear lobe, allows for mono-polar recording. The voltage differential between two electrodes placed on the scalp is captured during bipolar recording. In order to record electroencephalograms (EEGs), subjects will need to wear electrode caps while they see the stimuli for predetermined amounts of time. According to the 10/20 international electrode placement scheme, as illustrated in Figure 1 [30], the electrodes within the electrode cap should be positioned as indicated. To set the limit on the distances between nearby electrodes, we utilize the integers 10/20. The rule of thumb is that adjacent electrodes should be at least 10% and no more than from the skull's front to rear or left to right. Different lobes make up the brain. Each letter stands for one of the lobe positions.

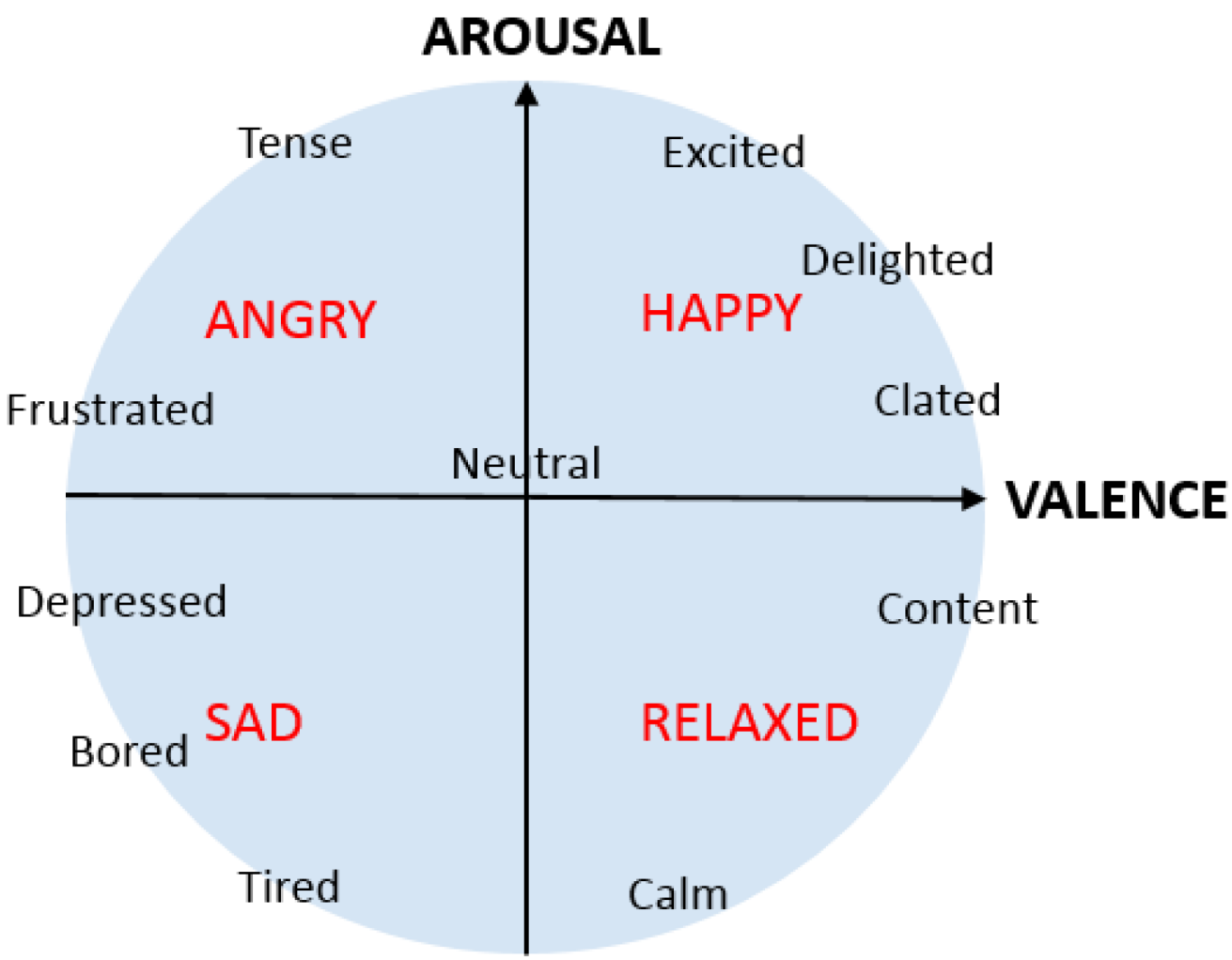

Figure 2. Valence-Arousal model of emotions [31]

B. Emotion representation

Both dimensional and category models can be used to represent emotions. ”Surprised” and ”Angry” are two examples of the types of emotions classified in the category model. A number of dimensions, , are used to describe emotions in dimensional models. Figure 2 displays the two-dimensional model that utilizes valence besides arousal [31]. In this valence-arousal space, emotions are labeled as individual points. Both the valence and arousal axes undergo a change, shifting from a negative to a positive state. The room in this mode is arranged in four equal halves. On the scale, which ranges from 1 to 9, valence and arousal levels are evaluated. Feelings like ”Excited” or ”Happy” (which are in the first quadrant) are possible when both the valence and arousal ratings are above 5. The second quadrant represents emotions like ”Angry” or ”Afraid” when valence is below 5 and arousal is above 5.

C. Feature extraction

The EEG’s intrinsic mode functions (IMF) reveal useful information on the signal’s temporal and frequency components. To calculate the IMFs of an EEG signal, the suggested approach makes use of EMD and VMD methods. Decomposing a signal into its constituent oscillatory parts yields what are known as IMFs. The two characteristics that are computed after obtaining the IMF signs of EEG data by VMD are the peak worth of the PSD and the first alteration of the signal.

1) Empirical mode decomposition (EMD)

In EMD, sifting is a repeated procedure that yields the IMFs of a signal s(t). There are two requirements that an IMF must meet. The first is that there can be no more than one difference among the sum of zero crossings and the extrema. Then, the upper enclose that is defined by local maxima and the lower envelop that is distinct by minima

both have zero mean values. The following are the full procedures to locate IMF:
1. Discovery out all minima and maxima in s(t).
2. Using envelop $env_{max}(T)$ and lower enclose $env_{min}(T)$ by least correspondingly.
3. Compute the mean of $env_{max}(T)$ and $env_{min}(T)$ as $m(t) = [env_{max}(T)+env_{min}(T)]/2$ and mean value is subtracted from the unique signal s(t). to get the particulars as d(t)=s(t)-m(t).
4. Cide whether d(t). satisfy the two basic circumstances of IMF.
5. To get first IMF I(t), recurrence the above ladders from (a) to (e) until it contents the obligatory two conditions of IMF.
Now sign d(t) will be the first IMF i.e I(t)=d(t),. . . ,or or next IMF, compute the residue x(t)=s(t)-I(t). This remainder will be named as a novel signal.
Now above steps will be repeated again.
6. The entire procedure will be sustained pending the residue discontinuing criteria (Say, it becomes constant). The unique signal in terms of its rotten IMF mechanisms is shown in Equation (1).

$$s(t) = \sum_{i=1}^{k} I_i(t) + x_k(t) \tag{1}$$

In the sum of IMFs got and $I_i(t)$ is the ith IMF. A example of six IMFs gotten using EMD is exposed in Figure 3.

2) Variational-Mode-Decomposition (VMD)

One method that uses time-frequency decomposition is VMD. Its purpose is to get around the following problems using EMD:
1. Because it employs a recursive method, EMD cannot rectify errors in the reverse direction.
2. It has trouble dealing with loud noises.

VMD use a concurrent technique rather than a recursive one. This adaptive approach takes the input signal and breaks it down into k independent modulation fields (IMFs), each of which has its own set of modes. The initial signal is represented by the total of these modes. When compared to EMD, VMD is less noise sensitive and produces no residual noise.
Finding IMFs is seen as an optimization issue in VMD. To decrease the total bandwidth of IMFs to a level where the total of all u_k equals the main signal, this is the goal of the optimization process. Figure 4 shows a trial of three IMFs that were produced using VMD.

D. Feature Selection using GRFO Algorithm

By employing the GRFO method for feature selection, we may enhance the classification outcomes. The Garra Rufa fish's unique "fish rubbing assembly" motion which involves swimming between two underwater legs provides the inspiration for GRFO, a novel optimization method [32]. Particles are categorized here, and the best one is chosen from each category. Based on the fitness of their group leader, some of these particles are given the ability to rearrange the group. The quantity of fish in each group determines how mobile those groupings are. The fish are organized into several groups, and each group has its own strategy for locating the system's operating point, which they use to locate food. Each group has a leader and a number of followers, or particles, of about the same size.
Each repetition, the followers switch groups based on the value. In this study, we assess the reference in the integrated EEG classification method by using the GRFO method. The following is how the GRFO method operates:
Step 1: Istarting: At the beginning of the process, the values of the voltages, currents, besides load demands are set up.
Step 2: Random cohort: The matrix generates the initialised parameter at random.
Step 3: The following is the procedure for doing a fitness calculation based on the system's objectives:.

$$F_i = Min(e) \tag{2}$$

To restore the system parameter in accordance with the Fitness Function (FF), the error function is denoted by e here.
Step 4: Set the limit to resort: The FF states that the system's limits are sorted.
Step 5: Verify the cycle. Make sure you've reached the maximum iteration and the best reference values. While the predicted number has an optimal point for the objective technique, the sum of leaders utilized in the selection process upsurges the problem's complexity. It is preferable to pay the optimal tariff between the fish passes from one group to another. In that case, we go back to the previous steps after completing the maximum number of iterations.
Step 6: Upgrade the limit: Increase the number of particles in each of the groups according to the definitions below.

$$N_f = \frac{n - N_L}{N_L} \tag{3}$$

In Equation (3), n represents the complete sum of particles, N_f demonstrations the sum of characterized followers, and N_L designates the sum of leaders.
Step 7: Make a list of the top and worst leaders. Here is the definition of the worst leader:

$$N_f = int(\alpha * rand) \tag{4}$$

$$m_{ij} = max((m_{ij-1} - N_f), 0) \tag{5}$$

Now, m_{ij} represents the leader. The best favorite is distinct as follows.

$$N_1 = \sum_{2}^{n} N_i \tag{6}$$

$$m_{1j} = m_{1d-1} - +N_1 \tag{7}$$

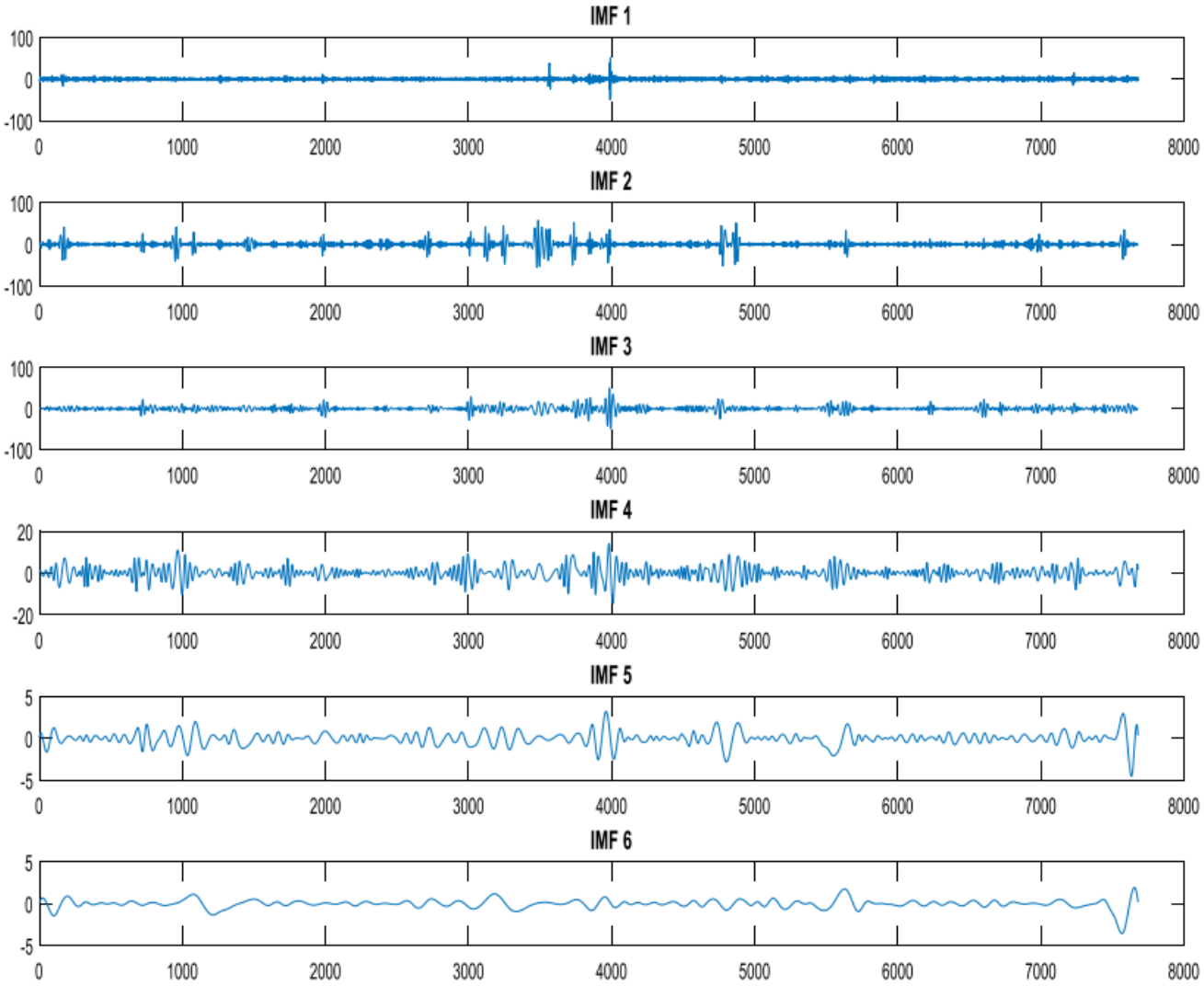

Figure 3. First six IMFs using EMD

Step 8: Strengthen both the position and the pace. Here we find the definitions of position and velocity.

$$v_i(t+1) = \omega v_i(t) + c_1 R_1(p_i(t) - X_i(t)) + c_2 R_2(g_i(t) - X_i(t)) \quad (8)$$

$$X_i(t+1) = X_i(t) + v_i(t+1) \quad (9)$$

In these expressions, V_i i-th atom, w characterizes the idleness mass limit, and c_1, and c_2 let the shown. Once the equations have been updated, the loop is linked to Phase 3. Both the accuracy of the classifier and the quantity of characteristics chosen are taken into account by the FF. It improves classification accuracy while reducing the size of the collection of characteristics used for selection. Consequently, the FF is employed to evaluate the specific solution in the following manner:

$$Fitness = a * ErrorRate + (1-a) * \frac{\#SF}{\#ALL\_F} \quad (10)$$

The classifier's error rate is now shown via ErrorRate. ErrorRate is a numerical value between 0 and 1 that represents the proportion of incorrect classifications relative to the total sum of classifications.In the original dataset, $\#SF$ indicates the selected features whereas $\#All\_F$ denotes all characteristics. The classifier's quality and subset length may be controlled using a. The value of an is taken to be 0.9 in this experiment.

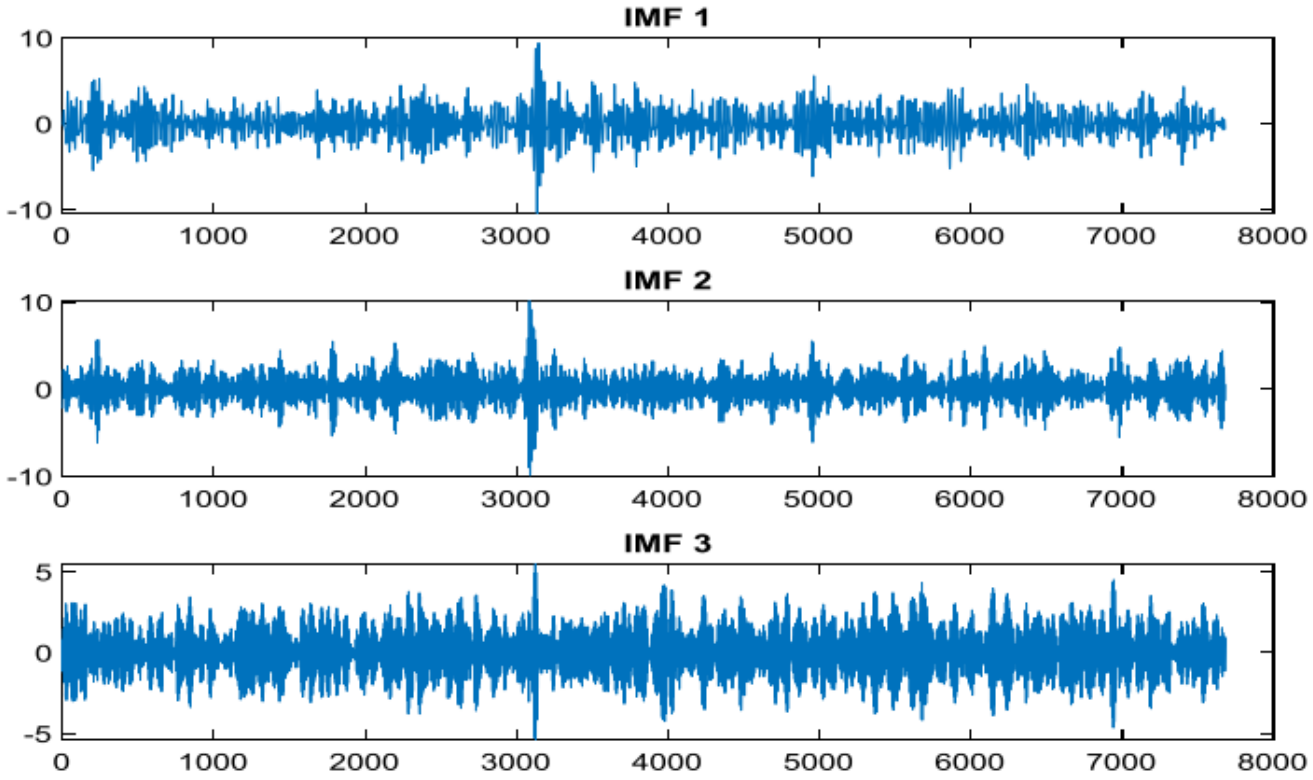

Figure 4. Primary three IMFs using VMD (electrode fp1 of valence class)

E. Classification using Ensemble Classifier with Voting Mechanism.

1) Extreme learning machine

Considering a set of N training samples $(X_i, t_i), i = 1, \ldots, N$ for m emotion classes, where each sample and its consistent label vector are correspondingly as $X_i = [X_{i1}, X_{i2}, \cdots X_{id}]^T \in R^d$ and $t_i = [t_{i1}, t_{i2}, \cdots t_{im}]^T \in R^m$. For ELM with multi-output nodes, if x_i belongs to the class m, the label vector is denoted as $t_i = [0, \cdots, 1, \cdots, 0]^T$. In ELM, the weights σ and biases $\square$ used to calculate the network outputs are both randomly generated and fixed. It is attainable by finding a solution to function, the goals of which are to decrease output weights while simultaneously achieving the least training error.

$$Minimize : L_p = \frac{1}{2}\|\beta\|^2 C\frac{1}{2}\sum_{n=1}^{N}\xi_i^2 \tag{11}$$

$$Subject \quad to : \quad h(X_i)\beta = t_i^T - \xi_i^T, i = 1, 2, ..., N$$

The data is mapped from layer feature space by any nonlinear activation function denoted as **j**. The ELM classifier's output function is based on the Karush-Kuhn-Tucker theorem.

$$\begin{aligned} f(X_i) &= h(X_i)\beta = h(X_i)H^T(\frac{1}{C} + HH^T)^{-1} \\ or &= h(X_i)(\frac{1}{C} + HH^T)^{-1}H^T T \end{aligned} \tag{12}$$

For any testing sample **y**, let $f_j(y)$ denote the consequence of the jth output node, i.e. $f(y) = [f_1(y), \ldots, f_m(y)]^T$, then the foretold class of trial **y** is

$$class(y) = arg^{max}_{i\in\{1,\cdots,m\}} f_i(y) \tag{13}$$

The hidden-layer activation functions in ELM can be almost any nonlinear piecewise continuous function, provided that the feature mapping **j** is known. Output functions from hidden layers often take the form of Sigmoid and Gaussian curves. We can use Mercer's conditions on ELM if **j** is not known. The definition of a kernel matrix is

$$\Omega_{ELM} = HH^T : \Omega_{ELM}(X_i, X_j) = h(X_i)h(X_j)^T = K(X_i X_j) \tag{14}$$

Then, Equation (12) can be written compactly as,

$$f(X_i) = h(X_i)H^T(\frac{1}{C}+HH^T)^{-1}T = \begin{bmatrix} K(X_i, X_1) \\ 4 \\ K(X_i, X_N) \end{bmatrix}(\frac{1}{C}+\Omega_{ELM})^{-1}T \tag{15}$$

It is clear from Equation (15) that the input data and the sum of training tasters are the only variables that affect the kernel form of the ELM classifier. You are also not need to provide the dimensionality **O** of space, which is the quantity of hidden nodes.

2) Multi-layer perception network

When it comes to classification tasks, MLP is often the artificial neural network of choice. For EEG-based AER, we compared ELM and MLP, two deep learning methods. The input, hidden, and output layers). As an input vector, MLP received the DE feature retrieved from the pre-processed EEG data. Various models were evaluated to confirm the accuracy of the recognition. The DE feature dimension for MLP was 160 input nodes, while the hidden node count ranged from 1 to 2 across 128, 64, 32, 16. For the best classification results, we used two hidden layers with one hundred and twenty-eight nodes and sixteen nodes, respectively.

3) Temporal convolutional network

Sequential data is often modelled using Convolutional Neural Networks (CNNs) and variants of them, such as Temporal Convolutional Networks (TCNs) [33]. To achieve a broad temporal receptive field with a small number of parameters, TCN uses dilated 1-D convolutions. The time dependency of different resolutions from the sequential data may be captured by blocks with varying dilation factors. In order to preserve low-level information and offer optimization hooks, each block contains a residual connection between its input and output. Not only that, but TCN's calculations may be executed in parallel, which drastically cuts down on model size while also speeding up training. We calculated the model parameters of a TCN with four eight dilation variables to examine the impact of various TCN configurations on speech separation.

4) Voting Mechanism

A thorough analysis of the combined results follows an exhaustive review of each model. Furthermore, a modified voting classifier, depicted in Figure 5, is a tailored application of heterogeneous Ensemble Learning (EL), and some shortcomings are also reduced.

Due to the wide variety of foundation models that make up the EL method, it may be said that it is heterogeneous. The goal of implementing the max voting method is to make DL classifiers more efficient. The first algorithm shows how to use the ensemble method of modified majority voting. Here, for each testing instance, the vote counter keeps track of the total number of votes cast by all of the algorithms in that category and saves them in CF. Then, the category with the greatest frequency value is described by the final prediction FPrei. As described in lines 16–21 of Algorithm 1, class probability is used to handle issues like the occurrence of two or more categories with the same frequency. The smart voting coordinator gets around these restrictions, as shown in Figure 5, by getting the greatest frequency value from the votes accumulated by the vote counter and using it as the final output. Then, the intelligent elective coordinator uses a brute-force method to thoroughly evaluate every possible mixture of the underlying base learners. Wherein a pair consists of exactly two basic learners, the absolute minimum. A strong and precise end forecast is guaranteed by such coordinated strategy.

Algorithm 1: Adapted Majority Voting Ensemble Procedure

Input: List of base replicas and BMk; Test data TDi
Output: Final forecast (FPrei) based on test data TDi

1 Model predictions dictionary,MPre: = f_g
2 Class probability dictionary,MPrePro: = f_g
3 Class frequencies,CF: = f_g
4 for each BMk do
5 Predict test data TDi
6 Store prediction results in MPre with the model name
7 Store class probability in MPrePro
8 end
9 for each MPre do
10 Extract the predicted class from MPre
11 Increment CF
12 end
13 Determine the class CLj,that occurs most frequently in CF
14 if frequencies are similar for two or more classes then
15 Sum up the class probability in MPrePro for the class CL_j
16 Update,FPrei CL_j for the TDi when the class probability is maximum
17 if class probabilities are similar for two or more classes then
18 Update,FPrei CL_j/ $*$ CL_j accepts an overall maximum occurrences in prediction results MPre */
19 end
20 end
21 Update,FPrei CLj for the TDi
22 Return FPrei

Algorithm 1 labels the DL representations used in this study.

4. Results and discussions

On a PC with a configuration of i5-8600k, GeForce 250GB SSD, besides 1TB HDD, the suggested model was tested using the Python 3.6.5 tool. Here are the parameters set: activation, ReLU, learning rate, batch size, epoch count, and dropout: 0.01.

A. Datasets

A Database for Emotion Investigation [34] besides a affect acknowledgement (HCI)2 [35] are two publically accessible benchmark datasets that we used to perform many experiments in order to assess the suggested ensemble model. The two datasets utilized in our research are summarized in Table I. Both datasets were used with arousal

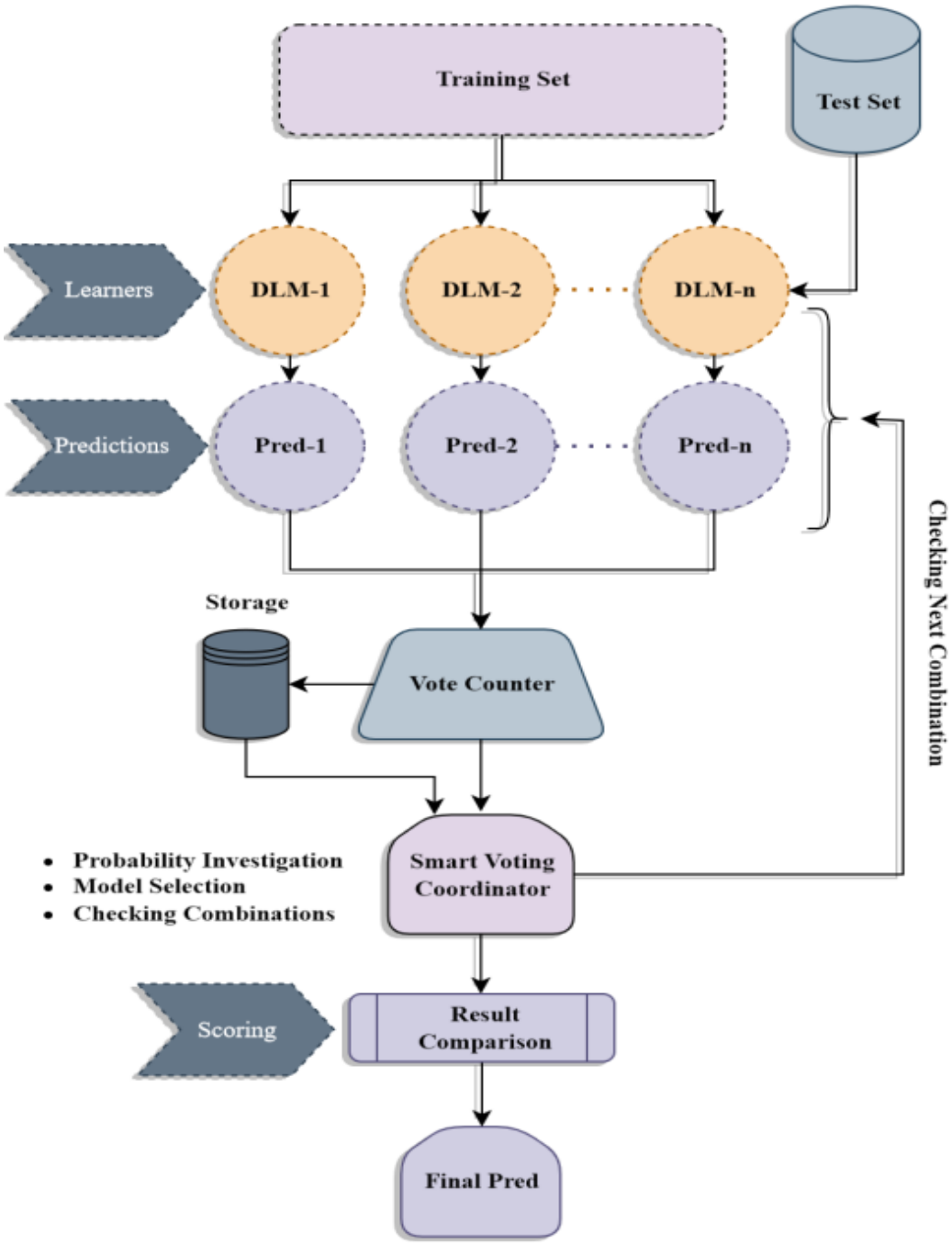

Figure 5. Functioning of the projected majority voting ensemble procedure

TABLE I. Swift of Related Evidence of the Datasets Used in the Researches

Factor	MAHNOB-HCI	DEAP
Subjects	27	32
Stimuli	Emotional videos	Music videos
Hearings/subject	20	40
Trial period	35-117s	1 min
EEG stations	32	32
Sampling rate	256Hz	512Hz
Label	V/A	V/A

and valence dimensions according to what was published in [36], [37], [38], [39].

DEAP is a dataset that includes several modalities of human emotional states, such as galvanic skin response (GSR), facial expressions, and (EEG). A total of thirty-two participants had their EEG, facial expression, and GSR monitored as they viewed music video clips. The total number of trials that each person takes part in is forty. With a 3-second baseline, each trial lasts for 1 minute. Arousal, liking are four dimensions of emotion with nine distinct levels each; after each trial, the respondent will fill out a questionnaire about their on these dimensions. With a sample rate using a 32-channel device. Another multi-modal dataset that is comparable to DEAP is MAHNOB-HCI. A total of thirty participants had their facial expressions, audio data, electroencephalogram (EEG), signals collected as they watched movie excerpts. It should be noted that subjects 12, 15, and 26 did not complete the data collection; so, this study utilized data from the remaining 27 out of 30 patients. The length of the video snippets ranges from 35 to 117 seconds. The 10-20 international system collects EEG readings from 32 electrodes. There are 256 hertz in the sample. The valence, arousal, dominance, and emotional keywords for each trial are labeled using four integers from 1 to 9, respectively, and the individuals self-report these values.

B. Pre-Processing

Every trial's DEAP baseline—three seconds long—was eliminated. The electrooculogram (EOG) was then eliminated using a separation technique after data downsampling from 512 Hz to 128 Hz. The original EEG was subjected to 4.0 to 45 Hz in order to eliminate the high- and low-frequency noise. The last step was to average the reference. Because the possible class labels for each dimension range from 1 to 9, we chose 5 as the cutoff for dividing the 9 values into high and low categories for each dimension, as previously mentioned [36]. Due to the vast number of trainable parameters in deep neural networks, a considerable amount of labeled data samples is necessary for optimal learning of emotion state representations in EEG. Nevertheless, the chosen datasets have a remarkably low number of trials (Table I). As a data augmentation step, we divided 4s chunks to get around this problem. Once the segments were prepared, the deep neural network was trained. With the following exception, MAHNOB-HCI's pre-processing was quite similar to that of the DEAP dataset. In order to make the remaining time correlate to the emotion elicitation event, we first deleted the 30-second from each trial. A band-pass filter reaching from 0.3 to 45 Hz was then functional to the initial EEG in order to eliminate the low- and high- noise. It should be noted that the part of an person's emotional state, therefore it is included.

C. Validation Analysis of proposed model

Here, the two datasets are used for validation and consequences are mentioned in Table II.

In above Table II represent that the Experimental study of various models. In the analysis of LR model attained the training accuracy as 0.874 and testing accuracy as 0.865 and testing loss of 0.219 besides testing loss of 0.235 and precision of 0.869 and recall of 0.862 besides f1-score as 0.865 correspondingly. Then the DBN classical attained the training accuracy as 0.842 and testing accuracy as 0.834and training loss of 0.289 and testing loss of 0.305 and precision as 0.836 and recall of 0.828 and f1-score as 0.833 correspondingly. Then the AE model attained the training accuracy as 0.901 besides testing accuracy as 0.896 and testing loss of 0.898 and recall of 0.891 and f1-score as 0.895 congruently. Then the XGBoost model accomplished the training accuracy as 0.892 and testing accuracy as 0.881 and testing loss of 0.167 besides testing loss of 0.178 and precision by way of 0.888 and recall of 0.876 besides f1-score as 0.882 correspondingly. Then the ELM model conquered the training accuracy as 0.854 and testing accuracy as 0.843 and testing loss of 0.271 and precision as 0.848 and recall of 0.839 and f1-score as 0.843 correspondingly. Then the MLP accuracy as 0.928 and testing accuracy as 0.916 0.084 and testing loss of 0.102 and precision as 0.912 and recall of 0.918 and f1-score as 0.915 similarly. Then the TCNN model accomplished the training accuracy as 0.903 and testing accuracy as 0.895 and testing loss of 0.898 and precision as 0.891 and f1-score as 0.894 similarly. Then the Ensemble Classifier model accomplished the training accuracy as 0.996 and testing accuracy as 0.0003 and testing loss of 0.0035 and precision as 0.992 and memory of 0.989 besides f1-score as 0.9764 correspondingly.

D. Experimental analysis of Feature Selection

Table III indicates that the Scrutiny of Projected GR-FOA. In the breakdown of 60-40% ratio, the precision as 0.889 and recall of 0.945 and accuracy as 90.48 besides f1-score as 0.916 and AUC ROC as 0.9 and AUC P-R as 0.932 correspondingly. Then 80-20% ratio, the precision as 0.958 and recall of 0.963 and accuracy as 98.92 and f1-score as 0.96 and AUC ROC as 0.978 and AUC P-R as 0.963 correspondingly. Then 70-30% ratio, the precision as 0.929 and recall of 0.986 and accuracy as 93.84 besides f1-score as 0.957 and AUC ROC as 0.909 and AUC P-R as 0.962 correspondingly.

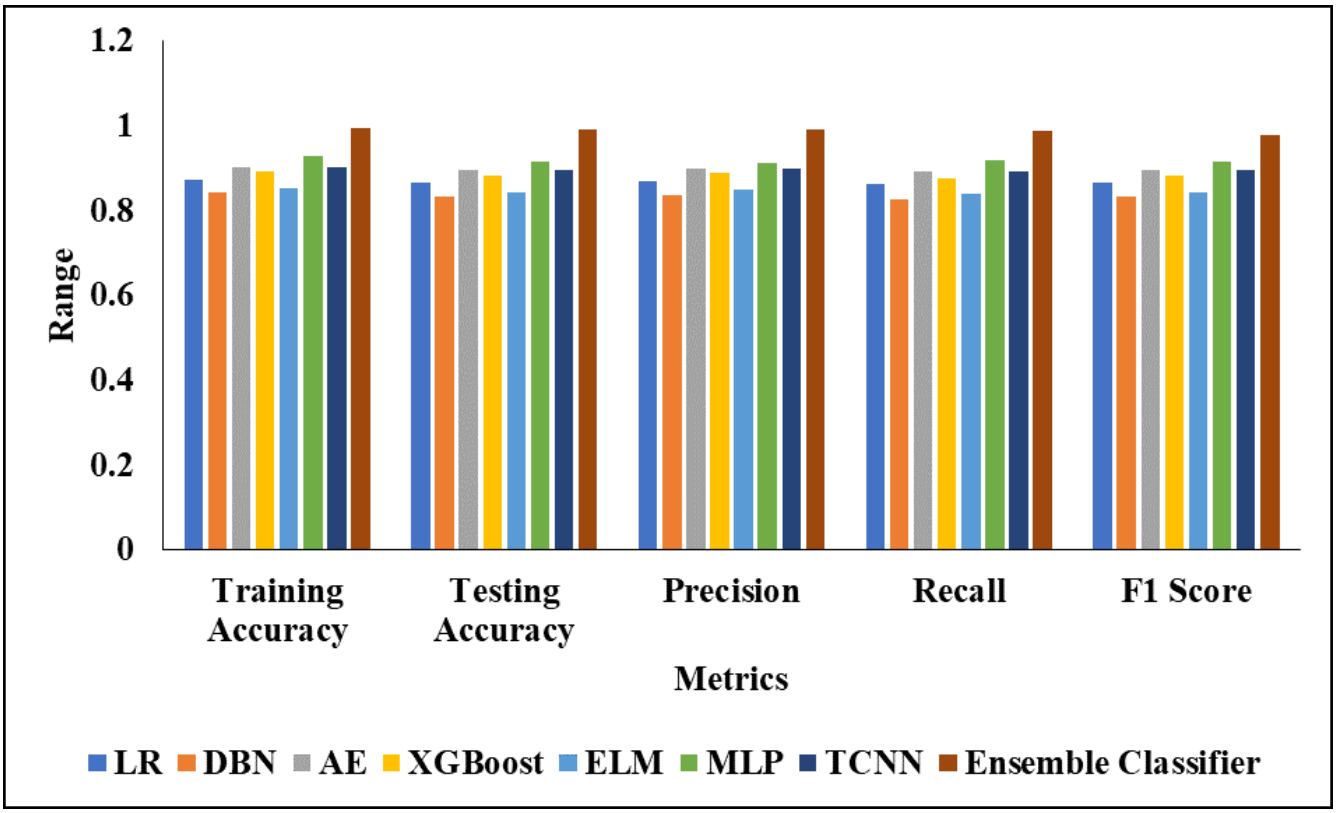

Figure 6. Graphical analysis of Proposed model

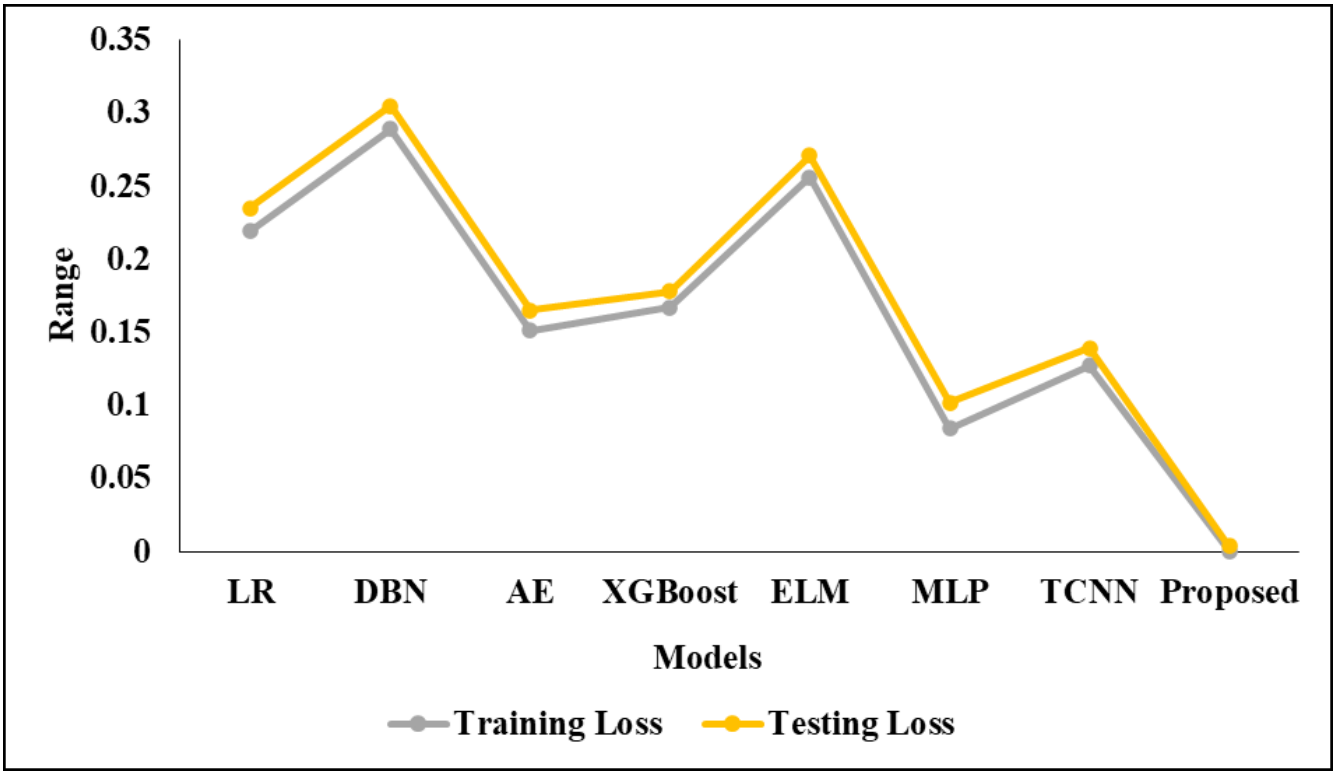

Figure 7. Visual Representation of various model

TABLE II. Experimental investigation of various models

Model Used	Training Accuracy	Testing Accuracy	Training Loss	Testing Loss	Precision	Recall	F1 Score
LR	0.874	0.865	0.219	0.235	0.869	0.862	0.865
DBN	0.842	0.834	0.289	0.305	0.836	0.828	0.833
AE	0.901	0.896	0.151	0.165	0.898	0.891	0.895
XGBoost	0.892	0.881	0.167	0.178	0.888	0.876	0.882
ELM	0.854	0.843	0.256	0.271	0.848	0.839	0.843
MLP	0.928	0.916	0.084	0.102	0.912	0.918	0.915
TCNN	0.903	0.895	0.127	0.139	0.898	0.891	0.894
Ensemble Classifier	0.996	0.991	0.0003	0.0035	0.992	0.989	0.9764

TABLE III. Analysis of Proposed GRFOA

Training-testing (%)	Precision	Recall	Accuracy	F1	AUC ROC	AUC P-R
60-40%	0.889	0.945	90.48	0.916	0.9	0.932
80-20%	0.958	0.963	98.92	0.96	0.978	0.963
70-30%	0.929	0.986	93.84	0.957	0.909	0.962

5. Conclusion

This research presents an EEG-based emotion identification system that is independent of the individual. The suggested approach uses EMD and VMD, which are employed for emotion categorization, to calculate IMFs. Two approaches, EMD besides VMD, are rummage-sale to extract EEG data. In order to classify EEG signals, the GRFOA model employs ensemble classifiers and handles the feature selection process. The ensemble model was evaluated on two publicly accessible MAHNOB-HCI, and it incorporates ELM, MLP, and TCNN models. The suggested approach is a global emotion detection system as it uses diverse participants' EEG data for model construction and testing. Therefore, the suggested approach may be used to the EEG of slightly individual employed for classifier training, allowing for emotion identification. To potentially enhance the prediction accuracy of comparable data, we want to modify the input data and employ soft clustering as a preprocessing step in the near future. Modifying the model also makes it applicable to all situations. In applications such as sleep monitoring, exercise intention, illness detection, and more, it can analyze and identify EEG data.

References

[1] M. Z. I. Ahmed, N. Sinha, S. Phadikar, and E. Ghaderpour, "Automated feature extraction on asmap for emotion classification using eeg," *Sensors*, vol. 22, no. 6, 2022. [Online]. Available: https://www.mdpi.com/1424-8220/22/6/2346

[2] X. Li, Y. Zhang, P. Tiwari, D. Song, B. Hu, M. Yang, Z. Zhao, N. Kumar, and P. Marttinen, "Eeg based emotion recognition: A tutorial and review," vol. 55, no. 4, 2022. [Online]. Available: https://doi.org/10.1145/3524499

[3] R. Agarwal, M. Andujar, and S. Canavan, "Classification of emotions using eeg activity associated with different areas of the brain," *Pattern Recognition Letters*, vol. 162, pp. 71–80, 2022. [Online]. Available: https://www.sciencedirect.com/science/article/pii/S016786552200263X

[4] S. Chatterjee and Y.-C. Byun, "Eeg-based emotion classification using stacking ensemble approach," *Sensors*, vol. 22, no. 21, 2022. [Online]. Available: https://www.mdpi.com/1424-8220/22/21/8550

[5] X. Zhu, W. Rong, L. Zhao, Z. He, Q. Yang, J. Sun, and G. Liu, "Eeg emotion classification network based on attention fusion of multi-channel band features," *Sensors*, vol. 22, no. 14, 2022. [Online]. Available: https://www.mdpi.com/1424-8220/22/14/5252

[6] E. Deniz, N. Sobahi, N. Omar, A. Sengur, and U. R. Acharya, "Automated robust human emotion classification system using hybrid eeg features with icbraindb dataset," *Health information science and systems*, vol. 10, no. 1, p. 31, December 2022. [Online]. Available: https://europepmc.org/articles/PMC9649575

[7] H. Liu, J. Zhang, Q. Liu, and J. Cao, "Minimum spanning tree based graph neural network for emotion classification using eeg," *Neural networks : the official journal of the International Neural Network Society*, vol. 145, pp. 308–318, 2021. [Online]. Available: https://api.semanticscholar.org/CorpusID:243467028

[8] D. Dadebayev, W. W. Goh, and E. X. Tan, "Eeg-based emotion recognition: Review of commercial eeg devices and machine learning techniques," *Journal of King Saud University - Computer and Information Sciences*, vol. 34, no. 7, pp. 4385–4401, 2022. [Online]. Available: https://www.sciencedirect.com/science/article/pii/S1319157821000732

[9] A. Thirumalraj, A. K, R. V, and P. K. Balasubramanian, "Designing a modified grey wolf optimizer based cyclegan model for eeg mi classification in bci," *Applied Soft Computing Journal*, 2023.

[10] A. Sakalle, P. Tomar, H. Bhardwaj, A. Iqbal, M. Sakalle, A. Bhardwaj, and W. Ibrahim, "Genetic programming-based feature selection for emotion classification using eeg signal," *Journal of Healthcare Engineering*, vol. 2022, 2022. [Online]. Available: https://api.semanticscholar.org/CorpusID:247368966

[11] B. Chakravarthi, S.-C. Ng, M. Ezilarasan, and M.-F. Leung, "Eeg-based emotion recognition using hybrid cnn and lstm classification," *Frontiers in computational neuroscience*, vol. 16, p. 1019776, 2022. [Online]. Available: https://europepmc.org/articles/PMC9585893

[12] Q. Gao, Y. Yang, Q. Kang, Z. Tian, and Y. Song, "Eeg-based

emotion recognition with feature fusion networks," . *International journal of machine learning and cybernetics*, vol. 13, no. 2, 2022.

[13] X. Wu, W.-L. Zheng, Z. Li, and B.-L. Lu, "Investigating eeg-based functional connectivity patterns for multimodal emotion recognition," *Journal of Neural Engineering*, vol. 19, 2020. [Online]. Available: https://api.semanticscholar.org/CorpusID:214802006

[14] J. Chen, T. Ro, and Z. Zhu, "Emotion recognition with audio, video, eeg, and emg: A dataset and baseline approaches," *IEEE Access*, vol. 10, pp. 13 229–13 242, 2022.

[15] N. Kumari, S. Anwar, and V. Bhattacharjee, "Time series-dependent feature of eeg signals for improved visually evoked emotion classification using emotioncapsnet," *Neural Computing and Applications*, vol. 34, pp. 13 291 – 13 303, 2022. [Online]. Available: https://api.semanticscholar.org/CorpusID:246740197

[16] M. A. Asghar, M. J. Khan, M. Rizwan, M. Shorfuzzaman, and R. M. Mehmood, "Ai inspired eeg-based spatial feature selection method using multivariate empirical mode decomposition for emotion classification," *Multimedia systems*, vol. 28, no. 4, p. 1275—1288, 2022. [Online]. Available: https://europepmc.org/articles/PMC8057947

[17] L. Yang, Q. Tang, Z. Chen, S. Zhang, Y. Mu, Y. Yan, P. Xu, D. Yao, F. Li, and C. Li, "Eeg based emotion recognition by hierarchical bayesian spectral regression framework," *Journal of Neuroscience Methods*, vol. 402, p. 110015, 2024. [Online]. Available: https://www.sciencedirect.com/science/article/pii/S0165027023002340

[18] M. Asif, N. Ali, S. Mishra, A. Dandawate, and U. S. Tiwary, "Deep fuzzy framework for emotion recognition using eeg signals and emotion representation in type-2 fuzzy vad space," *ArXiv*, vol. abs/2401.07892, 2024. [Online]. Available: https://api.semanticscholar.org/CorpusID:266998703

[19] C. Li, N. Bian, Z. Zhao, H. Wang, and B. W. Schuller, "Multi-view domain-adaptive representation learning for eeg-based emotion recognition," *Information Fusion*, vol. 104, p. 102156, 2024. [Online]. Available: https://www.sciencedirect.com/science/article/pii/S1566253523004724

[20] M. Akhand, M. A. Maria, M. A. S. Kamal, and T. Shimamura, "Emotion recognition from eeg signal enhancing feature map using partial mutual information," *Biomedical Signal Processing and Control*, vol. 88, p. 105691, 2024. [Online]. Available: https://www.sciencedirect.com/science/article/pii/S1746809423011242

[21] L. Farokhah, R. Sarno, and C. Fatichah, "Eeg-based emotion classification: A biologically informed channel selection approach," *International Journal of Intelligent Engineering and Systems*, vol. 17, no. 1, pp. 856–868, 2024, publisher Copyright: © (2024), (Intelligent Network and Systems Society). All Rights Reserved.

[22] M. A. Blanco-Rios, M. O. Candela-Leal, C. Orozco-Romo, P. Remis-Serna, C. S. Velez-Saboya, J. D.-J. Lozoya-Santos, M. Cebral-Loureda, and M. A. Ramirez-Moreno, "Real-time eeg-based emotion recognition model using principal component analysis and tree-based models for neurohumanities," 2024.

[23] J. Chen, X. Lin, W. Ma, Y. Wang, and W. Tang, "Eeg-based emotion recognition for road accidents in a simulated driving environment," *Biomedical Signal Processing and Control*, vol. 87, p. 105411, 2024. [Online]. Available: https://www.sciencedirect.com/science/article/pii/S1746809423008443

[24] C. Fan, H. Xie, J. Tao, Y. Li, G. Pei, T. Li, and Z. Lv, "Icaps-reslstm: Improved capsule network and residual lstm for eeg emotion recognition," *Biomedical Signal Processing and Control*, vol. 87, 2024. [Online]. Available: https://www.sciencedirect.com/science/article/pii/S1746809423008558

[25] J. Chang, Z. Zhang, Z. Wang, J. Li, L. Meng, and P. Lin, "Generative listener eeg for speech emotion recognition using generative adversarial networks with compressed sensing," *IEEE Journal of Biomedical and Health Informatics*, vol. 28, no. 2025-2036, 2024. [Online]. Available: https://ieeexplore.ieee.org/document/10416653

[26] R. Yuvaraj, P. Thagavel, J. Thomas, J. S. Fogarty, and F. Ali, "Comprehensive analysis of feature extraction methods for emotion recognition from multichannel eeg recordings," *Sensors (Basel, Switzerland)*, vol. 23, 2023. [Online]. Available: https://api.semanticscholar.org/CorpusID:255908111

[27] P. Dutta, S. Paul, K. Cengiz, R. Anand, and A. Kumar, "Chapter 2 - a predictive method for emotional sentiment analysis by deep learning from eeg of brainwave dataset," in *Artificial Intelligence for Neurological Disorders*, A. Abraham, S. Dash, S. K. Pani, and L. García-Hernández, Eds. Academic Press, 2023, pp. 25–48. [Online]. Available: https://www.sciencedirect.com/science/article/pii/B978032390277900002X

[28] S. Wang, J. Qu, Y. Zhang, and Y. Zhang, "Multimodal emotion recognition from eeg signals and facial expressions," *IEEE Access*, vol. 11, pp. 33 061–33 068, 2023.

[29] A. Iyer, S. S. Das, R. Teotia, S. Maheshwari, and R. R. Sharma, "Cnn and lstm based ensemble learning for human emotion recognition using eeg recordings," *Multimedia Tools and Applications*, vol. 82, pp. 4883–4896, 2022. [Online]. Available: https://api.semanticscholar.org/CorpusID:248113408

[30] J. N. Acharya, A. Hani, J. Cheek, P. Thirumala, and T. N. Tsuchida, "American clinical neurophysiology society guideline 2: Guidelines for standard electrode position nomenclature," *Journal of clinical neurophysiology : official publication of the American Electroencephalographic Society*, vol. 33, no. 4, p. 308—311, August 2016. [Online]. Available: https://doi.org/10.1097/WNP.0000000000000316

[31] P. Pandey and K. Seeja, "Subject independent emotion recognition from eeg using vmd and deep learning," *Journal of King Saud University - Computer and Information Sciences*, vol. 34, no. 5, pp. 1730–1738, 2022. [Online]. Available: https://www.sciencedirect.com/science/article/pii/S1319157819309991

[32] M. Maashi, B. Alabduallah, and F. Kouki, "Sustainable financial fraud detection using garra rufa fish optimization algorithm with ensemble deep learning," *Sustainability*, vol. 15, no. 18, 2023. [Online]. Available: https://www.mdpi.com/2071-1050/15/18/13301

[33] V. A. Thirumalraj, Arunadevi and B. P. Kavin., "An improved hunter-prey optimizer-based densenet model for classification of hyper-spectral images. in a. khang (ed.), ai and iot-based technologies for precision medicine," *IGI Global.*, 2023.

[34] S. Koelstra, C. Muhl, M. Soleymani, J.-S. Lee, A. Yazdani, T. Ebrahimi, T. Pun, A. Nijholt, and I. Patras, "Deap: A database for emotion analysis ;using physiological signals," *IEEE Transactions on Affective Computing*, vol. 3, no. 1, pp. 18–31, 2012.

[35] M. Soleymani, J. Lichtenauer, T. Pun, and M. Pantic, "A multimodal database for affect recognition and implicit tagging," *IEEE Transactions on Affective Computing*, vol. 3, no. 1, pp. 42–55, 2012.

[36] A. Appriou, A. Cichocki, and F. Lotte, "Modern machine-learning algorithms: For classifying cognitive and affective states from electroencephalography signals," *IEEE Systems, Man, and Cybernetics Magazine*, vol. 6, pp. 29–38, 2020. [Online]. Available: https://api.semanticscholar.org/CorpusID:220605514

[37] M. P. Kantipudi, N. S. P. Kumar, D. R. Aluvalu, S. Selvarajan, and K. Kotecha, "An improved gbso-taenn-based eeg signal classification model for epileptic seizure detection," *Scientific Reports*, vol. 14, 2024. [Online]. Available: https://api.semanticscholar.org/CorpusID:266845628

[38] M. A. Jabbar, M. P. Kantipudi, A. M. Madureira, M. B. I. Reaz, and S.-L. Peng, "Machine learning methods for signal, image and speech processing," *Machine Learning Methods for Signal, Image and Speech Processing*, 2022. [Online]. Available: https://api.semanticscholar.org/CorpusID:253072110

[39] D. R. Aluvalu, K. Aravinda, V. U. Maheswari, K. A. J. Kumar, B. V. Rao, and K. M. Prasad, "Designing a cognitive smart healthcare framework for seizure prediction using multimodal convolutional neural network," *Cognitive Neurodynamics*, pp. 1–13, 2024. [Online]. Available: https://api.semanticscholar.org/CorpusID:266726752

Author 1 short biography . . . . . .

Author 2 short biography . . . . . .

Author 3 short biography . . . . . .

Author 4 short biography . . . . . .

Author5 short biography . . . . . .

Author6 short biography . . . . . .